

Test study on the impact resistance of steel fiber reinforced full light-weight concrete beams

Yanmin Yang, Yunke Wang*, Yu Chen and Binlin Zhang

School of Civil Engineering, Jilin Jianzhu University, Changchun 130118, China

(Received August 1, 2019, Revised September 26, 2019, Accepted October 24, 2019)

Abstract. In order to investigate the dynamic impact resistance of steel fiber reinforced full light-weight concretes, we implemented drop weight impact test on a total of 6 reinforced beams with 0, 1 and 2% steel fiber volume fraction. The purpose of this test was to determine the failure modes of beams under different impact energies. Then, we compared and analyzed the time-history curves of impact force, midspan displacement and reinforcement strain. The obtained results indicated that the deformations of samples and their steel fibers were proportional to impact energy, impact force, and impact time. Within reasonable ranges of parameter values, the effects of impact size and impact time were similar for all volumetric contents of steel fibers, but they significantly affected the crack propagation mechanism and damage characteristics of samples. Increase of the volumetric contents of steel fibers not only effectively reduced the midspan displacement and reinforcement strain of concrete samples, but also inhibited crack initiation and propagation such that cracks were concentrated in the midspan areas of beams and the frequency of cracks at supports was reduced. As a result, the tensile strength and impact resistance of full light-weight concrete beams were significantly improved.

Keywords: steel fiber; full light-weight concrete; impact resistance; failure mode; midspan displacement; reinforcement strain

1. Introduction

During their service lives, engineering structures are affected by various impact loads, such as huge external impacts due to accidents, explosions, etc., resulting in serious, or even unrepairable, damages to the structures (Adhikary *et al.* 2015). As an important force-bearing member, when beam is subjected to severe explosive impact loads, its forced behavior greatly affects the overall impact resistance of the structure. Therefore, this paper studies the impact resistance of concrete beams.

Researchers from all over the world have conducted in-depth research on the mechanical properties of steel fiber reinforced concrete under cyclic loading. Tsonos (2009a, and 2009b) applied different types of concrete jackets to reinforce reinforced concrete structural specimens, and compared the seismic behavior of specimens by cyclic load test. The results indicated that steel fiber high-strength or ultra high-strength concrete jackets were proved to be much more effective than the reinforced concrete jackets and the FRP-jackets when used for the earthquake-resistant strengthening of reinforced concrete structural members. Structural members have better hysteresis performance, energy consumption and deformation ability, better failure modes. Chalioris (2013) and Chalioris *et al.* (2019) conducted cyclic loading tests on steel fiber reinforced concrete (SFRC) beams with different volume contents.

Test results indicated that the SFRC beams demonstrated improved overall hysteretic response, increased absorbed energy capacities, enhanced cracking patterns, and altered failure character from concrete crushing to a ductile flexural one compared to the RC beam. Steel fibres inhibit not only the development of cracking (crack propagation and crack width grow) but they also prevent cracks from closing during the reversal loading. Since testing of SFRC elements under cyclic deformations is very limited, the impact test of SFRC reinforced concrete beams is carried out.

Due to the high loading speed and short action time of impact load, the effect of material strain rate is significant. Researchers around the world have intensively studied the mechanical performance of concrete materials under impact loads (Fu *et al.* 1991, Malva *et al.* 1998). The brittleness of concrete is well-known and especially under the action of axial compression, its strain softening value is very low, which usually results in sudden burst failure. Recently, industrial experts and researchers have focused on steel fiber reinforced concretes. They have found that steel fibers increase the ductility of ordinary concretes and limit crack generation and development (Perumal *et al.* 2014, Lee *et al.* 2017). Wang *et al.* (2008) used $\phi=74$ mm split Hopkinson pressure bar (SHPB) to perform impact compression tests on high-strength concretes reinforced with ultrashort steel fibers with different volumetric contents, and determined the effect of the volumetric content and loading rate of steel fibers on concrete strength. The developed damage softening (SFRC) constitutive model was found to be consistent with the test results of high-strength concrete samples. Biolzi *et al.* (2017) improved the tensile strength and impact toughness of reinforced concrete beams by

*Corresponding author, Postgraduate
E-mail: 274895668@qq.com

adding steel fibers, which proved that steel fiber concrete beams have good ductility and energy dissipation. Yoo *et al.* (2015) studied the flexural behavior of SFRC beams under quasi-static and impact loads, and applied a drop-weight tester to impact tests on reinforced concrete beams with different steel fibers. Their results indicated that the increase of fiber content and strength leads to the enhancements in residual flexural performance of beams after impact damage. Fang *et al.* (2013) developed and validated a novel 3D concrete numerical calculation model, and used it to predict the dynamic response and destruction mode of steel fiber reinforced concrete samples under impact and explosive loads. Huo *et al.* (2017) compared the destruction modes of steel bar reinforced concrete beams with the same shear span ratios under static and drop weight impacts, and obtained the change laws of residual deformations of beams under impact loads. They concluded that, under high speed impact, beam cracks were mainly in the form of abdominal shear cracks.

At present, research on the impact response of steel fiber reinforced concrete components is mostly limited to ordinary concretes (Yoo *et al.* 2014, Amin *et al.* 2016, Hrynyk *et al.* 2014). Full light-weight concrete is an important class of lightweight aggregate concretes. It is a new building material with excellent properties such as light weight, high strength, environmentally friendliness, and good durability. Steel fibers are incorporated into full light-weight concrete to obtain steel fiber reinforced full light-weight concrete, which in addition to having the advantages of light weight coming from full light-weight concrete and good tensile due to steel fibers, it can effectively improve the static and dynamic performance of the final concrete sample. Based on the research on the mechanical properties of steel fiber reinforced full light-weight concretes, high performance drop weight testing system was applied to full light-weight concrete beams with different volumetric contents of steel fibers to carry out dynamic impact test. The aim of the test was to study the destruction mode of full light-weight concrete beams under impact. The influence of the volumetric contents and impact energies of steel fibers on the impact resistance of full light-weight concrete beams was studied by analyzing time-history curves of impact, midspan displacement and reinforcement strain.

2. Experimental

2.1 Materials

The cement used in this work was ordinary 42.5 model silicate cement. Light and coarse aggregates were made of shale ceramsite with particle size of 5-30 mm and light and fine aggregates were made of regional shale pottery soil with particle size of 3-4 mm. Wavy steel fibers had the length of 30 mm and diameter of 0.6 mm. The component materials are shown in Fig. 1. The longitudinal bars of beams was made of HRB400 grade steel, and stirrups were made of HPB300 grade round steel. The mixture ratios and mechanical performance indices of LC35 steel fiber reinforced full light-weight concrete samples are summarized in Tables 1 and 2, respectively.

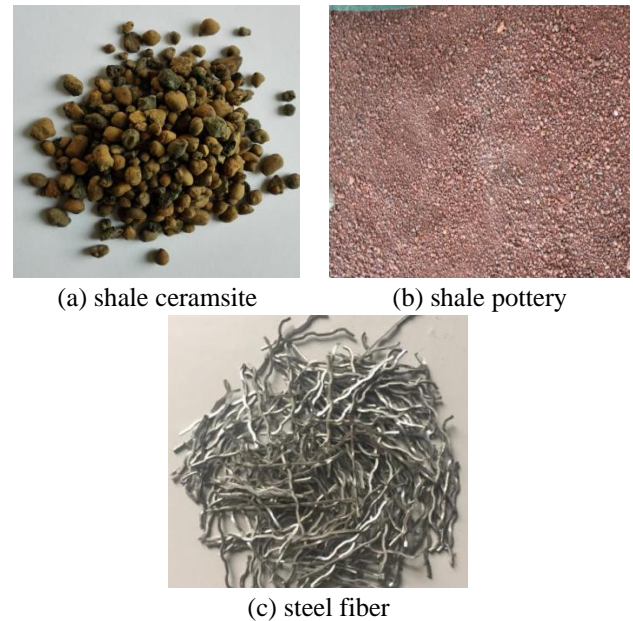


Fig. 1 Component materials

Table 1 The compositions of steel fiber reinforced full light-weight concretes

Sample No.	Volumetric content of steel fiber	cement (kg)	ceramsite (kg)	Shale pottery (kg)	Fly ash (kg)	Water reducer %	W/C
G0	0%	100	100	60	10	0.75	0.4
G1	1%	110	100	60	10	0.75	0.4
G2	2%	120	100	60	10	0.75	0.4

Table 2 Mechanical performance indices of steel fiber reinforced full light-weight concrete

Sample No.	Cube compressive pressure (MPa)	Axial compressive strength (MPa)	Elastic modulus (MPa)	Splitting tensile strength (MPa)	Rupture strength (MPa)	Dry apparent density (kg/m ³)
G0	37.5	35.7	1.96×10 ⁴	3.6	1.38	1559
G1	42.2	39.2	2.25×10 ⁴	6.6	4.66	
G2	45.9	42.2	2.33×10 ⁴	7.7	5.78	

2.2 Experimental design

A total of 6 full light-weight concrete reinforced beams with different steel fiber volumetric contents were fabricated in this work. Their protective layer thickness was 25 mm. The design parameters of steel fiber reinforced full light-weight concrete beams are shown in Table 3. The reinforcement is shown in Fig. 2.

2.3 Sample preparation

Sample production included the processing and lashing of steel bars, designing and production of mold, and casting and maintenance of concrete. In order to prevent the agglomeration of steel fibers and concrete mixture during the preparation of steel fiber reinforced full light-weight concrete samples, batch feeding mode was adopted to ensure the uniform distribution of steel fibers in concrete

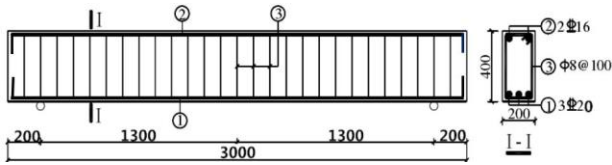


Fig. 2 The reinforcements of steel fiber reinforced full light-weight concrete beams

Table 3 The design parameters of beam samples

Sample No.	volumetric content of steel fiber	Concrete grade	Tensile steel bar	Compressive steel bar	Stirrup	Stirrup ratio
SFALCB-1	0%	LC35	2C16	3C20	Φ8@1000	5.03%
SFALCB-2						
SFALCB-3	1%					
SFALCB-4						
SFALCB-5	2%					
SFALCB-6						

Table 4 The parameters of drop weight system

Maximum impact drop (m)	Hammer weight range (kg)	Maximum impact energy (KJ)
16	187~1187	210

matrix (Nazarimofrad *et al.* 2017). The specific procedures followed those provided in CECS 13:89 “steel fiber concrete test method” (China Engineering Construction Standardization Association Standard 1989).

2.4 Loading plan

(1) High performance drop weight testing system was used to evaluate the effect of loading on concrete samples. The system was equipped with US NIPXI e-1006Q multi-channel data acquisition system capable of acquiring multi-channel high-speed synchronous voltage, acceleration and strain gauge signals. The system was equipped with a SONY high-speed camera which was capable of automatic synchronous high-speed photography. In the test, drop hammer and counterweight plate were lifted to a target height by a clamp, and were released to free fall along the guide rail to impact on the test samples. Beam support points were located at 200 mm from both ends of beams. Both upper and lower beam surfaces were equipped with sliding hinge supports fixed by pressure beam. The components and set up of test loading device is shown in Figs. 3 and 4, respectively, and the parameters of the drop weight system are summarized in Table 4.

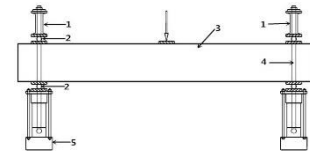
(2) The schematic diagram of data acquisition and test control systems are shown in Figs. 5 and 6, respectively. Hammer impact was collected by four strain gauges mounted on the upper part of the hammer. Strain signal was amplified by a strain amplifier and stored in oscilloscope for recording. High-speed camera (shooting rate of 800 frames per second) which was used to record the entire test process, is shown in Fig. 7.

(3) The effects of different steel fiber volumetric contents and impact energies on the impact resistance of full light-weight concrete beams were considered in the test.

Table 5 The parameters of loading test

Sample number	volumetric content of steel fibers	Hammer weight (kg)	Impact height (m)	Impact energy E(J)
SFALCB-1	0%	237	3.6	8361
SFALCB-2		387	3.6	13653
SFALCB-3	1%	287	4.8	13653
SFALCB-4		387	3.6	13653
SFALCB-5	2%	387	4.8	18204
SFALCB-6		387	3.6	13653

Note: Impact energies in the table were calculated as $E=mgh$ with $g=9.8m/s^2$, and h was the impact height of drop hammer



1. pressure beam 2. sliding hinge support 3. tested piece 4. tie rod 5. rigid support

Fig. 3 Test loading device



Fig. 4 Drop weight test set-up

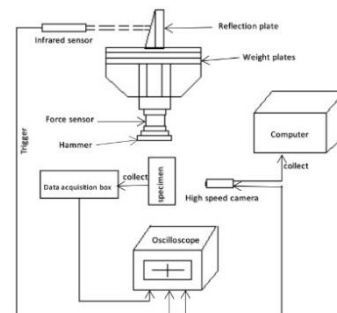


Fig. 5 The data acquisition system of drop weight testing

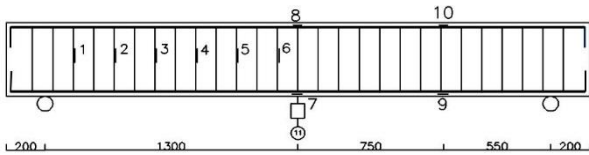


Fig. 6 The control system of drop weight testing

Impact energy was controlled by adjusting drop weight and impact height. The parameters of loading tests are summarized in Table 5.



Fig. 7 High-speed camera



1-6 are stirrup strain gauges, 7-10 are longitudinal bar strain gauges, and 11 is tie rod displacement sensor.

Fig. 8 Measuring point arrangement

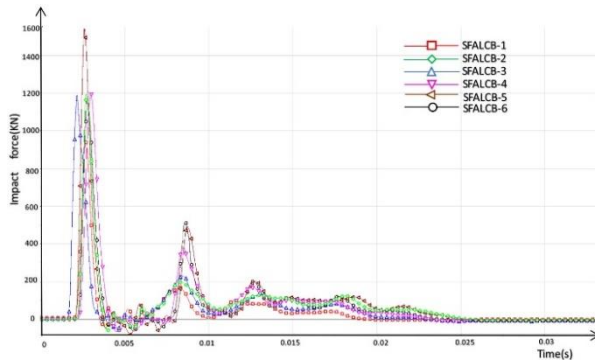


Fig. 9 Time-history curves of the impacts of different samples

2.5 Detection plan

Stirrup strain measuring points were selected at the half length of beams, and tie rod displacement sensors were employed to collect the time-history curves of beam midspan displacements. The measuring range of tie rod displacement sensors was 300 mm with the precision of 1 mm. Measuring point arrangement is shown in Fig. 8.

3. Results and discussion

3.1 Time-history curves of impacts

According to experimental loading scheme and measuring point arrangement, the generated impacts on test samples under loading were collected by force sensors installed on the upper part of the hammer. Figs. 9 and 10 show the time-history curves and impact durations of different samples, respectively. The maximum impact values of the test samples are listed in Table 6.

The impact curves of samples SFALCB-1 to 6 were basically the same. The impact of each test sample consisted of a main large pulse waveform and a few

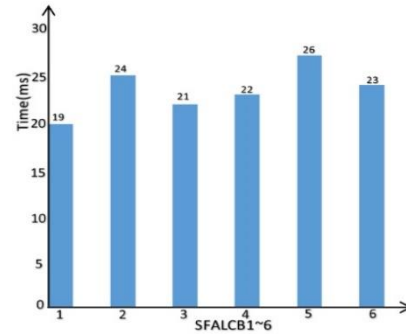


Fig. 10 Impact durations

Table 6 The maximum impact value (kN) of each test piece

SFALCB-1	SFALCB-2	SFALCB-3	SFALCB-4	SFALCB-5	SFALCB-6
963	1192	1184	1208	1581	1176

secondary smaller waves which complied with the results of Fujikake *et al.* (2009), Yoo *et al.* (2015) and proved the effectiveness of the proposed method. During the test, hammer head began to contact the sample at 0.002 s. At the moment of contact, the impact began to rise sharply and reached its maximum value in 0.001s. Then, the impact quickly returned to zero load position. Due to stress wave resistance, beams started to rebound after 0.004s. In addition, hammer head and full light-weight concrete beams showed multiple oscillations. Impact curve started to fluctuate up and down at zero load position. Finally, the impact tended to be stable at about 0.023 s.

(1) Based on different impact energies, samples SFALCB-1 and SFALCB-5 had the lowest and highest impact energy, impact peak and action time, respectively. Compared with SFALCB-6, when the impact energy of sample SFALCB-5 was increased by 4551J, the maximum impact value and impact action time were increased by 405 kN and 3ms, respectively. Therefore, impact energy had an obvious effect on impact peak and duration.

(2) Samples SFALCB-2, SFALCB-4 and SFALCB-6 had the steel fiber volumetric contents of 0, 1 and 2%, respectively. When impact energy was the same, the impact peak and duration of the three abovementioned test samples were basically the same, being 1200 kN and 22 ms. Therefore, it could be concluded that within the test parameters, steel fiber volumetric content did not have a meaningful effect on impact peak and duration. This is caused by the fact that since the first peak load under impact is closely related to the first cracking in the matrix, the first peak load is mainly influenced by the matrix cracking rather than the fiber bridging effect. This is consistent with the findings from Caverzan *et al.* (2012). that high strain-rates mostly influence in the peak strength related to the matrix properties and fiber debonding phase rather than the fiber pull-out (post-cracking) strength. Once a crack is formed, most of the applied load is resisted by the fibers at the crack surfaces. Therefore, the post-peak response is strongly influenced by the fiber content; the second peak load significantly increases as the fiber content increases. A similar observation was also reported by Dey *et al.* (2014). The peak load indicates the first cracking load in

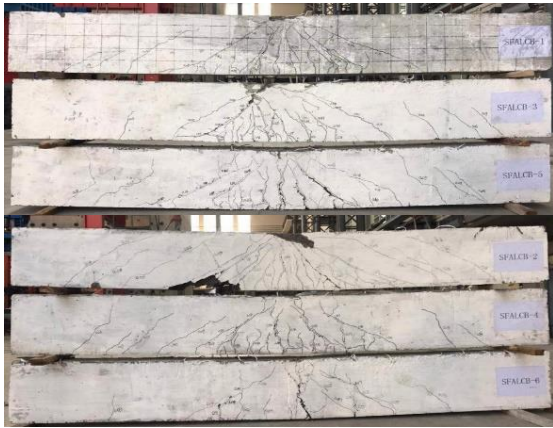


Fig. 11 failure modes of test samples

the SFRC full light-weight beams. Immediately after formation of the first cracking, the impact load steeply decreased. This is attributed to a load associated with kinetic energy imparted in fracturing the beam. If no fiber is included in the matrix, the impact load will decrease to zero, whereas if fibers are included in the matrix, the impact load will increase again with the fiber bridging effect, and after reaching second peak load, the load gradually decreased with fiber pull out. The second peak load was obviously influenced by the fiber bridging capacity.

3.2 Failure mode

Impact test was performed on 6 full light-weight

concrete beams by adjusting drop hammer weight and impact height. The 6 test samples were damaged to various degrees, and the whole process was recorded with a high-speed camera. The failure modes of all test samples under impact load are shown in Fig. 11. The impact damage process of samples SFALCB-2 and SFALCB-4 is shown in Fig. 12.

It can be seen from Fig. 11 that a wedge-shaped oblique crack similar to an isosceles triangle was generated at beam midspan and vertical cracks appeared on the wedge body, which were similar to results reported in Jin *et al.* (2017). At initial loading stage, the impact acted on beam midspan position, and bending fluctuations were observed in the beam. Then, the impact began to transfer from impact point to the support at both ends of the beam, and bending wave propagated to beam end points. Crack appearance order on beam surface was basically consistent with beam bending fluctuation. A large number of oblique and vertical cracks first appeared at beam midspan position; then oblique cracks began to appear on beam support with fewer numbers and lower widths. By further loading, lower oblique cracks on the beam midspan and vertical cracks were further developed and merged to form the main crack, and the number of cracks was further increased. At the same time, the cracks on the support were further developed but their number was significantly fewer than those in midspan area.

The impact energy of sample SFALCB-2 was about 1.6 times that of SFALCB-1. The cracks of SFALCB-1 were mainly concentrated at midspan position and were relatively small. The beam deformations of all full light-weight

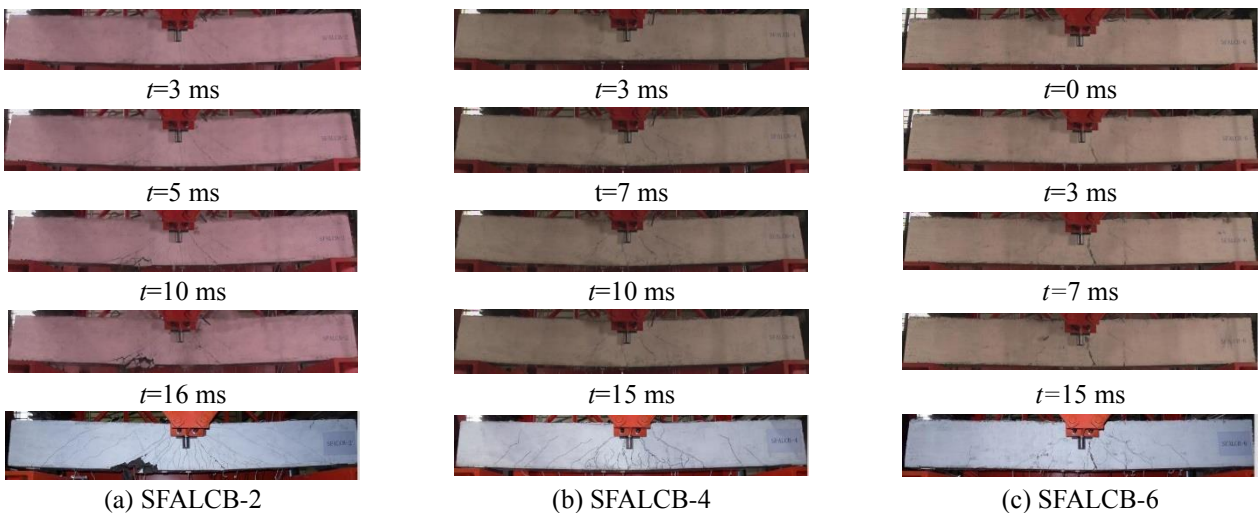


Fig. 12 The impact process of the samples SFALCB-2, SFALCB-4 and SFALCB-6



Fig. 13 Partial destructions of test samples

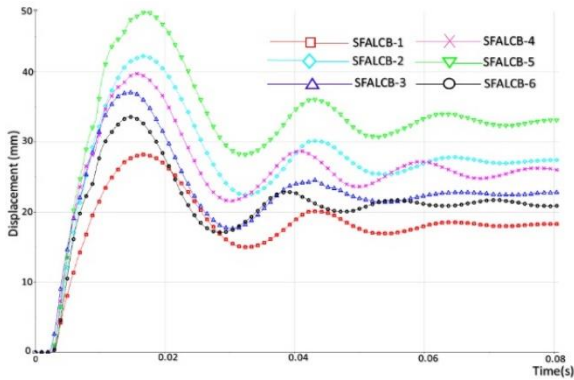


Fig. 14 Midspan displacement of test samples

concrete samples were small. However, the damage of SFALCB-2 was more serious than other samples and its concrete fell off. Midspan cracks were obvious in this sample which extended to support at both sides. Similarly, cracks on SFALCB-6 concentrated in a small area with a relatively wide main crack appearing only at midspan position. Cracks on both sides of this sample were few in number and relatively small and no cracks appeared at the ends of the support. In contrast, SFALCB-5 cracks occurred in a wide area and there were not only multiple wider main cracks at midspan position, but also a large number of cracks appeared on both sides of the sample and at both ends of the support.

Unlike SFALCB-2, SFALCB-4 and SFALCB-6, steel fibers were not incorporated into SFALCB-2 and its damage was the most serious. There was a large quantity of concrete fall off at the contact point of beam midspan and hammer. The fractured section of the crack was smooth and belonged to the brittle fracture of light aggregate. By incorporating 1% steel fiber into SFALCB-4, more cracks appeared on the beam. The cracks were mainly concentrated at midspan area, and those at both ends of the support were few in number and relatively small in size. Steel fibers were pulled out or broken at destruction surface, and fracture cross-section was not flat. By adding 2% steel fiber into SFALCB-6, the total number of cracks was decreased with obvious cracks appearing at midspan position and no cracks appearing at both ends of the support. Since steel fibers were connected to ceramsite in full light-weight concrete samples and steel fiber itself had a large tensile strength, full light-weight concrete beams were pulled out or off consuming a fraction of energy. Observing the samples SFALCB-2 and SFALCB-4 in Fig. 13, it can be seen that when the sample is loaded, a large number of vertical cracks and wedge-shaped oblique cracks appear in the middle of the beam span, and oblique cracks appear at the support. The failure mode of the beam body is characterized by obvious bending and shear failure modes. It can be seen from the failure phenomenon of the sample SFALCB-6 that when the sample is loaded, a vertical crack runs through the bottom of the beam in the span of the beam. As the crack further develops, the main crack is finally formed, and the beam body is obviously deflected downward. The phenomenon of curvature is equivalent to forming a plastic hinge in the beam span. At the same time, there are subtle

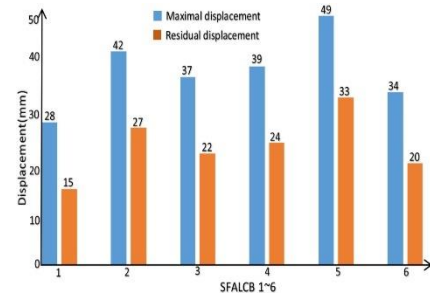


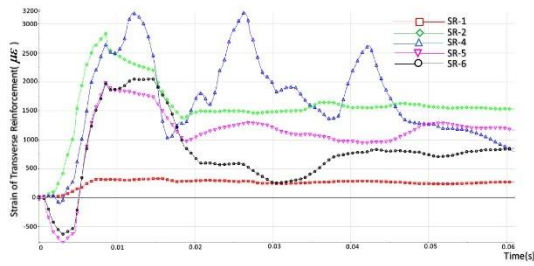
Fig. 15 Midspan maximum displacements and residual deformation of test samples

symmetrical oblique cracks around the beam span, and there are almost no cracks at the support. It can be seen from the crack occurrence area and crack development that the beam body is destroyed. Beam damage has obvious characteristics of bending damage. Ordinary concrete will exhibit brittle collapse when the tensile stress generated exceeds the ultimate strength of the tensile concrete. After the steel fiber concrete is cracked, Steel fibers have a tensile stress transfer capability on the crack surface that is significantly resistant to shearing of the developing crack. This phenomenon is also known as crack-bridging (Watanabe *et al.* 2010, Chalioris 2013). Thus, steel fibers have been proved as a promising non-conventional reinforcement in shear-critical concrete beams due to the advantageous cracking performance of SFRC and, under specific circumstances, could alter the brittle shear failures to ductile flexural ones. The potential partial replacement of common steel stirrups with fibers, especially in cases where design criteria recommend high transverse steel ratio that leads to short stirrup spacing has already been investigated (Chalioris *et al.* 2011, Tsonos 2014). Therefore, it was concluded that the addition of steel fibers effectively improved the tensile strength and especially ameliorates the post-cracking behavior of full light-weight concrete beams.

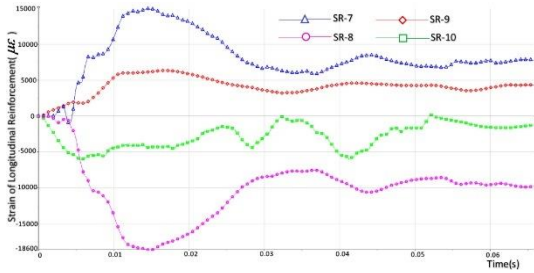
3.3 Time-history curves of midspan displacement

The voltage pulse signals collected by rod-type resistor displacement sensor were filtered with DIAdem data processing software and converted into displacement signals according to a certain proportional relationship. Fig. 14 shows time-history curves of midspan displacements of test samples. Fig. 15 shows the maximum displacements and residual deformations of midspan.

As can be observed in the time-history curves of test samples, the development trend of midspan displacement was basically the same for all samples. During test loading process, after hammer head contacted the beam, full light-weight concrete beams began to undergo deflection deformations and beam midspan displacements began to increase rapidly. The maximum value of midspan displacements was reached in about 0.015s. Then, beams began to rebound to equilibrium position and displacements began to decrease. Due to impact stress wave, beams started to vibrate and curves began to move in the form of sine waves and gradually decayed; finally, they were stabilized in about 0.07s. Stable position was considered to be the

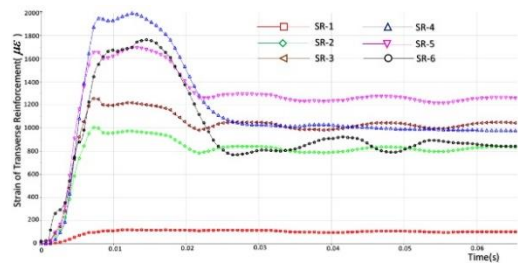


(a) Measuring point 1-6

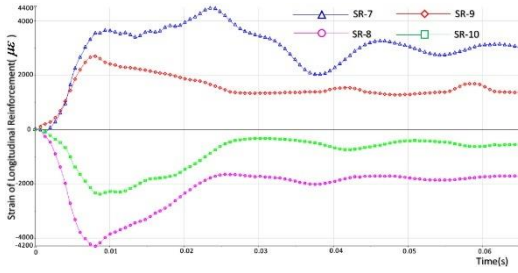


(b) Measuring point 7-10

Fig. 16 The reinforcement strain of SFALCB-2 sample

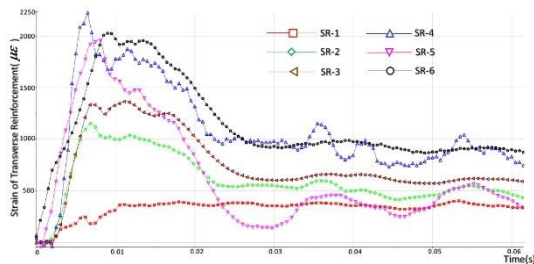


(a) Measuring point 1-6

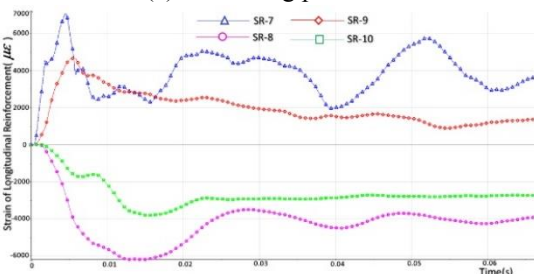


(b) Measuring point 7-10

Fig. 18 The reinforcement strain of SFALCB-6 sample



(a) Measuring point 1-6



(b) Measuring point 7-10

Fig. 17 The reinforcement strain of SFALCB-4 sample

residual displacement of test samples after impact.

Both midspan maximum displacements and residual deformations of test samples were increased with the increase of impact energy. Compared with SFALCB-1, the impact energy of SFALCB-2 was increased by 63.3%. and their midspan maximum displacements and residual deformations were increased by 50% and 80%, respectively. Similarly, Compared with SFALCB-6, the impact energy of SFALCB-5 was increased by 33.3% and their midspan maximum displacements and residual deformations were increased by 44% and 65%, respectively.

With the increase of steel fiber volumetric content, midspan maximum displacements and residual deformations of test samples were gradually decreased. Steel fiber volumetric contents of SFALCB-2, SFALCB-4 and SFALCB-6 samples were 0, 1 and 2%, respectively.

Their midspan maximum displacements were 42, 39 and 34 mm and their residual deformations were 27, 24, and 20 mm, respectively. Therefore, these factors were inversely proportional to steel fiber volumetric contents which was similar to the results reported in Bhatti *et al.* (2009), Lee *et al.* (2018).

3.4 Time-history curves of reinforcement strain

Taking the reinforcement strain curves of SFALCB-2, SFALCB-4 and SFALCB-6 as examples, the symbol SR represented the reinforcement strain gauge. The time-history curves of reinforcement strain are shown in Figs. 16, 17 and 18.

At the beginning of loading, the strains of most stirrups were suddenly increased, and concrete began to crack. The occurrence and development of cracks causes the concrete to no longer bear tensile stress. Then, the stress at crack points was mainly carried by steel bars. With the continuation of impact load, beam deformation and stirrup strain reached their maximum values. Because beams resisted against impact stress wave, they started to rebound to equilibrium position and stirrup strain was decreased rapidly. After stabilizing, strain was recorded as stirrup residual strain which was positive. Its value indicated that after the beam was subjected to impact load, stirrups in beams were in tension state. The trend of the longitudinal bar strain of test samples were basically the same. At initial loading stage, the strain of longitudinal bar was increased sharply, and then began to decrease and was gradually stabilized. The reinforcement strain of the upper beam was negative, while the reinforcement strain of the lower beam was positive, and that at midspan was significantly larger than that of half midspan position.

SR-1 was 140 mm away from support and its strain value was relatively small compared with other positions which indicated that shear stress was relatively small at this point; however, SR-4 was 770 mm away from support, and

its strain was the largest indicating that shear stress was the largest at this point. It can also be seen from the failure mode diagrams of test samples that oblique cracks occurred the most frequently and damage was the most serious at these positions. At the initial stage of the test, SR-4, SR-5, and SR-6 of SFALCB-2 and SFALCB-4 were both negative. This showed that steel bars at these positions were pressed at the moment of contact between hammer head and beam; this was more obvious in SFALCB-2 than SFALCB-4, while it was not witnessed in SFALCB-6. As steel fiber volumetric contents were increased, reinforcement strain peaks at the corresponding positions of each test sample were gradually decreased indicating that the increase of steel fiber volumetric content effectively increased beam stiffness and reduced beam deformation.

SR-7 was located at the lower part of the positive section of beam impact point, and received the highest impact load. Reinforcement strain was the largest and positive at this point which indicated that steel bars were in tension state. SR-9 was located at the semi-midspan position of the beam. Its bearing impact and steel strain were smaller than those at midspan position. Similarly, reinforcement strain at SR-8 was higher and negative, which indicated that steel bars were under pressure at this point and that at SR-10 was relatively small. In conclusion, by increasing steel fiber volumetric content, reinforcement strain peak and residual deformation at the corresponding positions of test samples were significantly reduced. It was demonstrated that increasing steel fiber volumetric content could effectively reduce reinforcement strain and increase the stiffness of full light-weight concrete beam.

4. Conclusions

In this study, 6 full light-weight concrete beams were subjected to drop weight impact test, and the crack distribution diagrams of steel fiber reinforced full light-weight concrete beams were obtained. We also obtained the time-history data of impact, midspan displacement and reinforcement strain. Moreover, we analyzed and summarized the effects of different variables on the impact resistance of test samples, and the following conclusions were drawn:

- Impact energy had a significant effect on impact peak and impact time. When impact energy was increased to 5292 and 9843J, impact peak was increased to 229 and 634 kN and impact time was increased to 5 and 7ms, respectively. This indicated that both impact peak and impact duration were increased with the increase of impact energy. The impact peak and action time of test samples with different steel fiber volumetric contents were basically the same which indicated that steel fiber volumetric contents did not affect impact peak and duration within the range of parameter values studied in this paper. But the post-peak response is strongly influenced by the fiber content; the second peak load significantly increases as the fiber content increases. The incorporation of steel fibers significantly increases the energy consumption and ductility of full light concrete beams.

- Under impact load, the partial damage degrees of test samples were proportional to impact energy and the width and development range of cracks in the samples. The increase of steel fiber volumetric content significantly reduced crack generation and development. It also changed the cracking form of the beam and made crack occurrence area relatively concentrated forming a vertical crack mainly concentrated at midspan position. The number of cracks near the support were relatively reduced and appeared as small oblique cracks.

- Impact energy had a significant effect on the midspan displacement of test samples. With the increase of the steel fiber volumetric contents of the beams, the maximum displacements and residual deformations of midspan points of test samples were gradually decreased. Under the same impact energy, when steel fiber volumetric content was increased by 1 and 2%, midspan maximum displacement was decreased by 3 and 8 mm, and residual displacement was decreased by 3 and 7 mm, respectively. This indicated that increasing steel fiber volumetric content enhanced concrete beam stiffness and reduced its deformation under loading.

- Under impact load, the denser the oblique crack was, the larger the stirrup strain of the more severely damaged area of full light-weight concrete beam became, the relatively smaller the stirrup strain near both ends of support was. Longitudinal bar strain was the largest at the midspan position of all test samples. As steel fiber volumetric contents of the samples were increased, stirrup and longitudinal bar strains were significantly reduced. This showed that increasing steel fiber volumetric contents effectively improved the stiffness of test samples and reduced their stirrup strain.

- The fractured section of full light-weight beam was smooth and belonged to the brittle fracture of light aggregate, and tensile strength was low. After the incorporation of steel fibers, cracks were developed along the direction of these fibers and they were pulled out or broken at the destruction surface and the section was not flat. The pulled out or broken steel fibers consumed a part of the energy which effectively enhanced the tensile strength and impact resistance, and especially ameliorates the post-cracking behavior of full light-weight concrete beams.

Acknowledgments

This research was supported by National Key Research and Development Plan (2017YFC0806100), National Emergency Management Department Safety Accident Prevention Science and Technology Project (jilin-0001-2018AQ) and Jilin Province Education Department Planning Project (JJKH20190872KJ).

References

- Adhikary, S.D., Li, B. and Fujikake, K. (2015), "Low velocity impact response of reinforced concrete beams: experimental and numerical investigation", *Int. J. Protect. Struct.*, **6**(1), 81-111.

- <https://doi.org/10.1260/2041-4196.6.1.81>.
- Amin, A. and Foster, S.J. (2016), "Shear strength of steel fibre reinforced concrete beams with stirrups", *Eng. Struct.*, **111**(5), 323-332. <https://doi.org/10.1016/j.engstruct.2015.12.026>.
- Bhatti, A.Q., Kishi, N., Mikami, H. and Ando, T. (2009), "Elasto-plastic impact response analysis of shear-failure-type rc beams with shear rebars", *Mater. Des.*, **30**(3), 502-510. <https://doi.org/10.1016/j.matdes.2008.05.068>.
- Biolzi, L. and Cattaneo, S. (2017), "Response of steel fiber reinforced high strength concrete beams: Experiments and code predictions", *Cement Concrete Compos.*, **77**, 1-13. <https://doi.org/10.1016/j.cemconcomp.2016.12.002>.
- Caverzan, A., Cadoni, E. and Di, P.M. (2012), "Tensile behaviour of high performance fibre-reinforced cementitious composites at high strain rates", *Int. J. Impact Eng.*, **45**, 28-38. <https://doi.org/10.1016/j.ijimpeng.2012.01.006>.
- Chalioris, C.E. (2013), "Analytical approach for the evaluation of minimum fibre factor required for steel fibrous concrete beams under combined shear and flexure", *Constr. Build. Mater.*, **43**, 317-336. <https://doi.org/10.1016/j.conbuildmat.2013.02.039>.
- Chalioris, C.E. (2013), "Steel fibrous RC beams subjected to cyclic deformations under predominant shear", *Eng. Struct.*, **49**, 104-118. <https://doi.org/10.1016/j.engstruct.2012.10.010>.
- Chalioris, C.E. and Sfiri, E.F. (2011), "Shear performance of steel fibrous concrete beams", *Procedia Eng.*, **14**, 2064-2068. <https://doi.org/10.1016/j.proeng.2011.07.259>.
- Chalioris, C.E., Kosmidou, P.K. and Karayannis, C.G. (2019), "Cyclic response of steel fiber reinforced concrete slender beams: An experimental study", *Mater.*, **12**(9), 1398. <https://doi.org/10.3390/ma12091398>.
- China Engineering Construction Standardization Association Standard (1989), *Test Methods for Steel Fiber Reinforced Concrete*, China Planning Press, Beijing, China. (in Chinese)
- Dey, V., Bonakdar, A. and Mobasher, B. (2014), "Low-velocity flexural impact response of fiber-reinforced aerated concrete", *Cement Concrete Compos.*, **49**, 100-110. <https://doi.org/10.1016/j.cemconcomp.2013.12.006>.
- Fang, Q. and Zhang, J. (2013), "Three-dimensional modelling of steel fiber reinforced concrete material under intense dynamic loading", *Constr. Build. Mater.*, **44**, 118-132. <https://doi.org/10.1016/j.conbuildmat.2013.02.067>.
- Fu, H.C., Erki, M.A. and Seckin, M. (1991), "Review of effects of loading rate on concrete in compression", *J. Struct. Eng.*, **117**(12), 3645-659. [https://doi.org/10.1061/\(ASCE\)0733-9445\(1991\)117:12\(3645\)](https://doi.org/10.1061/(ASCE)0733-9445(1991)117:12(3645)).
- Fujikake, K., Li, B. and Soeun, S. (2009), "Impact response of reinforced concrete beam and its analytical evaluation", *J. Struct. Eng.*, **135**(8), 938-950. [https://doi.org/10.1061/\(ASCE\)ST.1943-541X.0000039](https://doi.org/10.1061/(ASCE)ST.1943-541X.0000039).
- Hrynyk, T.D. and Vecchio, F.J. (2014), "Behavior of steel fiber-reinforced concrete slabs under impact load", *ACI Struct. J.*, **111**(5), 1213-1224.
- Huo, J.S. and Huo, K.Y. (2017), "Failure mechanism of rc beams under impact loading and discussion on prediction methods of residual deflection.", *J. Hunan Univ. (Nat. Sci.)*, **44**(1), 112-117. (in Chinese)
- Jin, L., Zhang, R.B., Dou, G.Q., Xu, J.D. and Du, X.L. (2017), "Experimental and numerical study of reinforced concrete beams with steel fibers subjected to impact loading", *Int. J. Damage Mech.*, **27**(7), 1058-1083. <https://doi.org/10.1177/1056789517721616>.
- Lee, J.H., Cho, B. and Choi, E. (2017), "Flexural capacity of fiber reinforced concrete with a consideration of concrete strength and fiber content", *Constr. Build. Mater.*, **138**, 222-231. <https://doi.org/10.1016/j.conbuildmat.2017.01.096>.
- Lee, J.Y., Shin, H.O., Yoo, D.Y. and Yoon, Y.S. (2018), "Structural response of steel-fiber-reinforced concrete beams under various loading rates", *Eng. Struct.*, **156**, 271-283. [tps://doi.org/10.1016/j.engstruct.2017.11.052](https://doi.org/10.1016/j.engstruct.2017.11.052).
- Malvar, L.J. and Ross, C.A. (1998), "Review of strain rate effects for concrete in tension", *ACI Struct. J.*, **95**(6), 735-739.
- Nazarimofrad, E., Shaikh, F.U.A. and Nili, M. (2017), "Effects of steel fibre and silica fume on impact behaviour of recycled aggregate concrete", *J. Sustain. Cement-Bas. Mater.*, **6**(1), 182-202. <https://doi.org/10.1080/21650373.2016.1230900>.
- Perumal, R. (2014), "Performance and modeling of high-performance steel fiber reinforced concrete under impact loads", *Comput. Concrete*, **13**(2), 255-270. <https://doi.org/10.12989/cac.2014.13.2.255>.
- Tsonos, A.G. (2009a), "Steel fiber high-strength reinforced concrete: a new solution for earthquake strengthening of old R/C structures", *WIT Tran. Built Environ.*, **104**, 153-164.
- Tsonos, A.G. (2009b), "Ultra-high-performance fiber reinforced concrete: an innovative solution for strengthening old R/C structures and for improving the FRP strengthening method", *WIT Tran. Eng. Sci.*, **64**, 273-284.
- Tsonos, A.G. (2014), "A new method for earthquake strengthening of old R/C structures without the use of conventional reinforcement", *Struct. Eng. Mech.*, **52**(2), 391-403. <http://dx.doi.org/10.12989/sem.2014.52.2.391>.
- Wang, Z.L., Liu, Y.S. and Shen, R.F. (2008), "Stress-strain relationship of steel fiber-reinforced concrete under dynamic compression", *Constr. Build. Mater.*, **22**(5), 811-819. <https://doi.org/10.1016/j.conbuildmat.2007.01.005>.
- Watanabe, K., Kimura, T. and Niwa, J. (2010), "Synergetic effect of steel fibers and shear-reinforcing bars on the shear-resistance mechanisms of RC linear members", *Constr. Build. Mater.*, **24**(12), 2369-2375. <https://doi.org/10.1016/j.conbuildmat.2010.05.009>.
- Yoo, D.Y. and Yoon, Y.S. (2014), "Influence of steel fibers and fiber-reinforced polymers on the impact resistance of one-way concrete slabs", *J. Compos. Mater.*, **48**(06), 695-706. <https://doi.org/10.1177/0021998313477167>.
- Yoo, D.Y., Banthia, N., Kim, S.W. and Yoon, Y.S. (2015), "Response of ultra-high-performance fiber-reinforced concrete beams with continuous steel reinforcement subjected to low-velocity impact loading", *Compos. Struct.*, **126**, 233-245. <https://doi.org/10.1016/j.compstruct.2015.02.058>.
- Yoo, D.Y., Yoon, Y.S. and Banthia, N. (2015), "Flexural response of steel-fiber-reinforced concrete beams: effects of strength, fiber content, and strain-rate", *Cement Concrete Compos.*, **64**(2), 84-92. <https://doi.org/10.1016/j.cemconcomp.2015.10.001>.

AT